

<https://doi.org/10.1038/s43247-026-03244-1>

# Linking ecological resilience and ecosystem services to inform spatial conservation planning

Check for updates

Zhuangzhuang Wang <sup>1</sup>, Bojie Fu <sup>2,3,4</sup> ✉, Xutong Wu <sup>5</sup>, Shuai Wang <sup>5</sup>, Junze Zhang <sup>2</sup>, Liwei Zhang<sup>1</sup>, Lei Jiao<sup>1</sup>, Hao Wang<sup>1</sup>, Yingjie Li <sup>6</sup> & Ying Luo<sup>1</sup>

Balancing ecosystem service provision with long-term ecosystem stability remains a critical challenge for sustainable land management. Here, we develop a spatial planning framework that integrates ecological resilience—the capacity of an ecosystem to recover from perturbations—with ecosystem services to identify priority areas for ecological restoration. Applying this framework to the Loess Plateau of China, we evaluate three management strategies—Service Priority, Balanced Priority, and Resilience Priority—to delineate restoration priorities. Our results indicate that ecosystem services have generally improved from 2000 to 2020, while resilience exhibits a turning point, shifting from an increasing to a declining trend. Spatial overlay analyses further show that areas with enhanced ecosystem service supply coincide with declining resilience, indicating a spatial mismatch between service gains and resilience loss. The three prioritization scenarios produce distinct spatial patterns, highlighting the importance of balanced strategies that reconcile short-term service gains with long-term ecosystem resilience to inform sustainable restoration and land management.

Terrestrial ecosystems can exhibit diverse responses to environmental change, ranging from gradual adjustments to abrupt, often irreversible shifts in structure and function<sup>1</sup>. These critical transitions have attracted increasing attention for their potential to fundamentally reconfigure ecosystem dynamics and trigger the sudden collapse of services vital to human well-being<sup>2</sup>. Evidence from diverse ecosystems suggests that such shifts are widespread under global change<sup>2</sup>. A loss of resilience—defined as the capacity of ecosystems to recover from perturbations—is widely recognized as a precursor to these transitions<sup>3,4</sup>. Consequently, monitoring resilience through Earth observation data has become a key research priority for anticipating potential transitions and supporting early intervention<sup>5</sup>.

Ecosystem services are the benefits that ecosystems provide to human societies, including provisioning, regulating, supporting, and cultural services<sup>6</sup>. While ecosystem service supply reflects the current output of ecological functioning, its long-term sustainability depends on underlying resilience<sup>7</sup>. A high level of ecosystem service supply does not guarantee continued functionality if resilience is declining<sup>1</sup>. For instance, prior to observed declines in forest carbon sequestration, increased slowing down of NDVI responses to small disturbances has been

identified as an early warning signal of forest mortality<sup>8</sup>. Moreover, although global net biome production has increased in recent decades, its interannual variability has also intensified—particularly in warmer regions experiencing greater temperature fluctuations—suggesting potential destabilization of the terrestrial carbon sink under climate change<sup>9</sup>. These findings highlight the importance of monitoring resilience trends as leading indicators for potential ecosystem service loss.

Spatial conservation prioritization frameworks provide practical and cost-effective tools for supporting targeted and adaptive ecosystem management<sup>10</sup>. Traditionally, many existing frameworks have focused on biodiversity conservation and ecosystem service optimization as their primary objectives<sup>11–13</sup>. In recent years, however, the importance of incorporating ecological resilience into conservation planning has been increasingly recognized<sup>14,15</sup>. Despite this growing attention, the development of operational frameworks that explicitly integrate resilience remains methodologically limited, largely due to the conceptual ambiguity and the inherent difficulty of quantifying resilience<sup>16</sup>. Advances in satellite observations and critical slowing down (CSD) indicators—such as temporal autocorrelation and variance—offer promising means to measure resilience and assess

<sup>1</sup>School of Geography and Tourism, Shaanxi Normal University, Xi'an, China. <sup>2</sup>State Key Laboratory of Regional and Urban Ecology, Research Center for Environmental Sciences, Chinese Academy of Sciences, Beijing, China. <sup>3</sup>National Observation and Research Station of Earth Critical Zone on the Loess Plateau in Shaanxi, Xi'an, China. <sup>4</sup>Shaanxi Yan'an Forest Ecosystem Observation and Research Station, Beijing, China. <sup>5</sup>State Key Laboratory of Earth Surface Processes and Resource Ecology, Faculty of Geographical Science, Beijing Normal University, Beijing, China. <sup>6</sup>Natural Capital Project, Stanford University, Stanford, CA, USA.

✉ e-mail: [bfu@rcees.ac.cn](mailto:bfu@rcees.ac.cn)

ecosystem stability<sup>2,5,17</sup>. These indicators detect slower recovery rates and increased fluctuations as systems approach critical transitions<sup>18</sup>, providing a quantitative basis for integrating resilience into spatial conservation decision-making. Linking ecological resilience with ecosystem services thus enables a more comprehensive and robust foundation for identifying priority areas under uncertain environmental conditions.

The Loess Plateau is an ecologically fragile region in China, characterized by severe soil erosion, land degradation, and livelihood vulnerability driven by high population pressure and sparse vegetation<sup>19,20</sup>. Since the launch of large-scale ecological restoration programs such as the Grain-for-Green Project in 1999, vegetation cover has increased markedly—from 31.6% to 67% by 2020—enhancing ecosystem services such as soil conservation and carbon sequestration<sup>21–23</sup>. However, emerging evidence suggests that high-density vegetation recovery has pushed the region toward the limits of its water-vegetation carrying capacity, exacerbating soil moisture depletion and raising concerns about the long-term sustainability of these ecological gains<sup>24,25</sup>. Consequently, conservation priorities are shifting from expanding vegetation cover to sustaining restoration outcomes and enhancing ecosystem resilience<sup>20</sup>. These characteristics make the Loess Plateau an ideal case for developing and testing resilience-based ecosystem service conservation planning.

In this study, we develop a spatially explicit framework to identify ecological conservation and restoration priority areas by integrating ecosystem service assessments with resilience indicators. Using the Loess Plateau as a case study, we aim to identify multifunctional yet vulnerable areas that require urgent conservation interventions. Specifically, we (1) quantify ecological resilience using CSD indicators derived from time-series

vegetation indices, (2) assess ecosystem services based on multi-source data and biophysical models, and (3) integrate resilience and ecosystem service metrics into a spatial optimization model to delineate conservation priority areas. Our results show that recent gains in ecosystem service supply in the Loess Plateau are accompanied by a decline in ecological resilience, leading to pronounced spatial mismatches between service provision and ecosystem resilience. These findings highlight the need for conservation prioritization strategies that balance ecosystem service enhancement with long-term resilience.

### Theoretical and technical framework

This study develops an integrated framework for identifying spatial conservation priorities by jointly considering ecological resilience and ecosystem services (Fig. 1). The framework builds on the ecosystem service cascade concept, which emphasizes that ecosystem structure and function—shaped by both climate change and human activities—jointly determine the supply and stability of ecosystem services essential for human well-being<sup>20,26,27</sup>. Declining ecological resilience increases the likelihood of critical transitions from healthy to degraded states, thereby threatening the sustained delivery of ecosystem services<sup>8</sup>. Thus, simultaneous monitoring of resilience and service supply is crucial for sustainable ecosystem management.

Within this framework, ecological resilience represents the capacity of ecosystems to recover from perturbations and was quantified using early-warning indicators from CSD theory<sup>2</sup>. As systems approach a tipping point, their recovery rate diminishes, reflected by increasing temporal autocorrelation and variance in ecological time series<sup>28</sup>. The kernel normalized difference vegetation index (kNDVI) was used as a proxy for vegetation

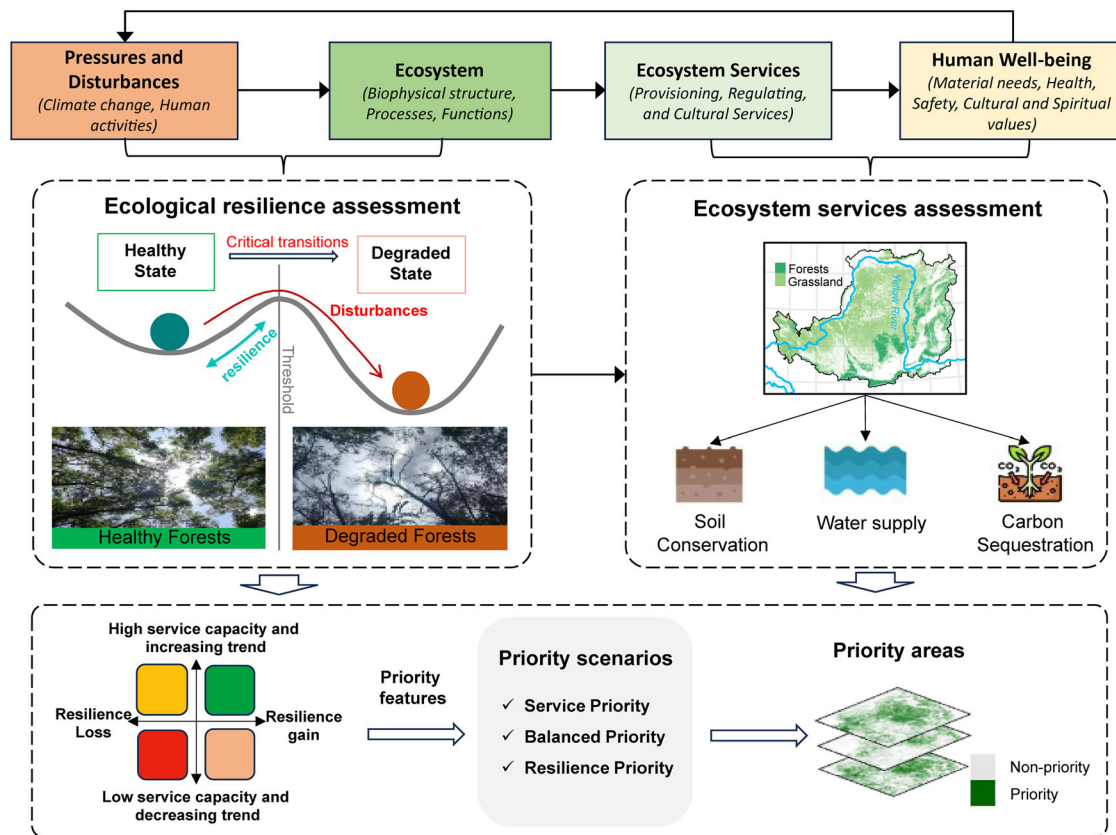


**Fig. 1 | Theoretical and technical framework linking ecological resilience and ecosystem services for spatial conservation planning.** The framework integrates resilience assessment (middle left panel) and ecosystem service assessment (middle right panel) to prioritize areas for management. The lower left panel illustrates four color-coded quadrants representing combinations of service capacity, service trends, and resilience dynamics: green = high capacity with service increase and resilience

gain; yellow = high capacity with service decrease and resilience loss; orange = low capacity with service increase and resilience gain; red = low capacity with service decrease and resilience loss. These quadrants define priority features that guide three conservation scenarios—service priority, resilience priority, and balanced priority—used to generate spatially explicit priority maps.

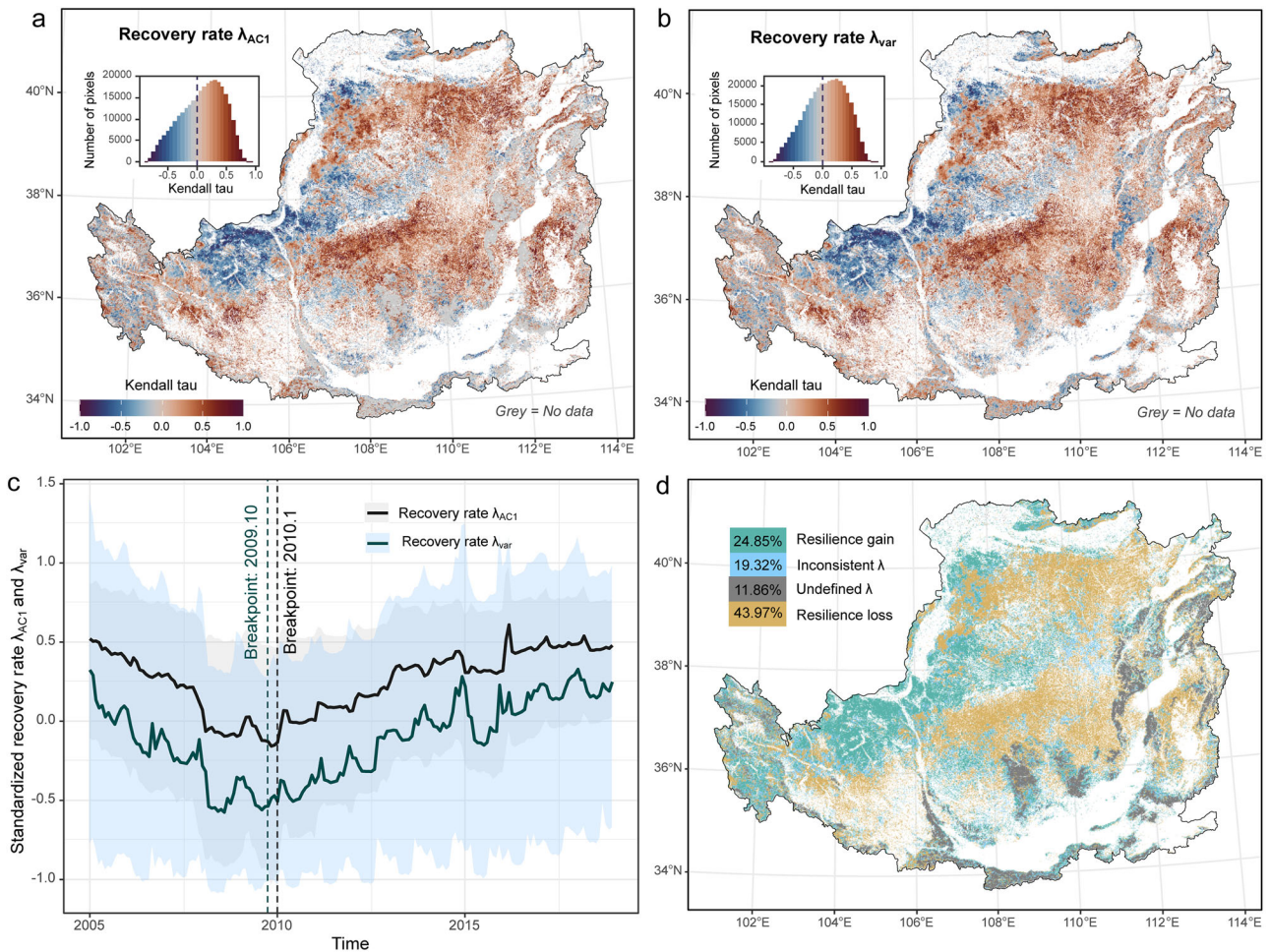


**Fig. 2 | Spatial patterns and temporal trends of ecological resilience on the Loess Plateau. a, b** Spatial pattern of Kendall’s tau trends in  $\lambda_{AC1}$  and  $\lambda_{var}$ ; histograms show the pixel count distributions. **c** The median standardized recovery rates  $\lambda_{AC1}$  and  $\lambda_{var}$ ; each value is plotted in the middle of the five-year moving window. Shaded

bands indicate the interquartile range (25th to 75th percentiles). **d** Integrated spatial classification of resilience change types based on the consistency of trends in  $\lambda_{AC1}$  and  $\lambda_{var}$ .

dynamics, serving as a consistent indicator of ecosystem responses across heterogeneous landscapes<sup>29</sup>.

Ecosystem services were quantified in parallel to represent the functional dimension of ecosystems. Three key services—soil conservation, water supply, and carbon sequestration—were selected to capture the dominant ecological processes of the Loess Plateau<sup>30</sup>. These services collectively reflect hydrological regulation, erosion control, and carbon storage functions that underpin regional sustainability.

By spatially integrating resilience and service assessments, the framework identifies areas where high service supply coincides with declining resilience, revealing potential spatial trade-offs. These trade-offs were further evaluated using a scenario-based spatial optimization model to delineate conservation and restoration priorities under three management strategies: Service Priority, Balanced Priority, and Resilience Priority. The resulting maps provide spatially explicit insights into how functionality and stability can be jointly optimized to support long-term ecological sustainability in the Loess Plateau and similar dryland ecosystems.

## Results

### Spatiotemporal dynamics of ecological resilience and ecosystem services

Both recovery rates derived from lag-1 autocorrelation ( $\lambda_{AC1}$ ) and variance ( $\lambda_{var}$ ) consistently show a widespread slowing down across the central and northern regions (Fig. 2a–b), indicating a regional decline in resilience. The standardized regional medians of both indicators declined markedly before

2010 and gradually increased thereafter (Fig. 2c). This temporal pattern suggests that resilience initially improved during the early phase of large-scale ecological restoration but began to decline around 2010. Sensitivity tests with alternative window combinations confirmed the robustness of the results (Supplementary Fig. 2–3).

Based on the consistency between  $\lambda_{AC1}$  and  $\lambda_{var}$  trends, resilience change was spatially categorized (Fig. 2d). Approximately 43.97% of the study area experienced resilience loss, primarily in the central and northern regions, while 24.85% showed resilience gains, mostly in the northwest. In contrast, 13.2% of the area displayed inconsistencies between  $\lambda_{AC1}$  and  $\lambda_{var}$  trends, making resilience change assessments less reliable in these regions. Furthermore, 11.86% of the area showed undefined recovery rates due to negative AC1 values, predominantly in dense forest ecosystems with high biomass. In these regions, the use of optical vegetation indices—even the improved kNDVI—may be constrained by signal saturation, which dampens temporal variability and reduces the sensitivity of CSD-based indicators<sup>29</sup>.

Over the past two decades, carbon sequestration increased significantly across 93.48% of the study area, and soil erosion decreased across 66.65% of the region (Fig. 3d, e). In contrast, most regions showed no significant trend in water supply (Fig. 3f), with areas of significant decrease (5.3%) slightly exceeding those of increase (3.59%). Multi-year averages of ecosystem service supply (Fig. 3a–c) reveal clear spatial heterogeneity across the Loess Plateau. Carbon sequestration and water supply capacity decrease gradually from the southeast to the northwest (Fig. 3a, c). In comparison, soil erosion

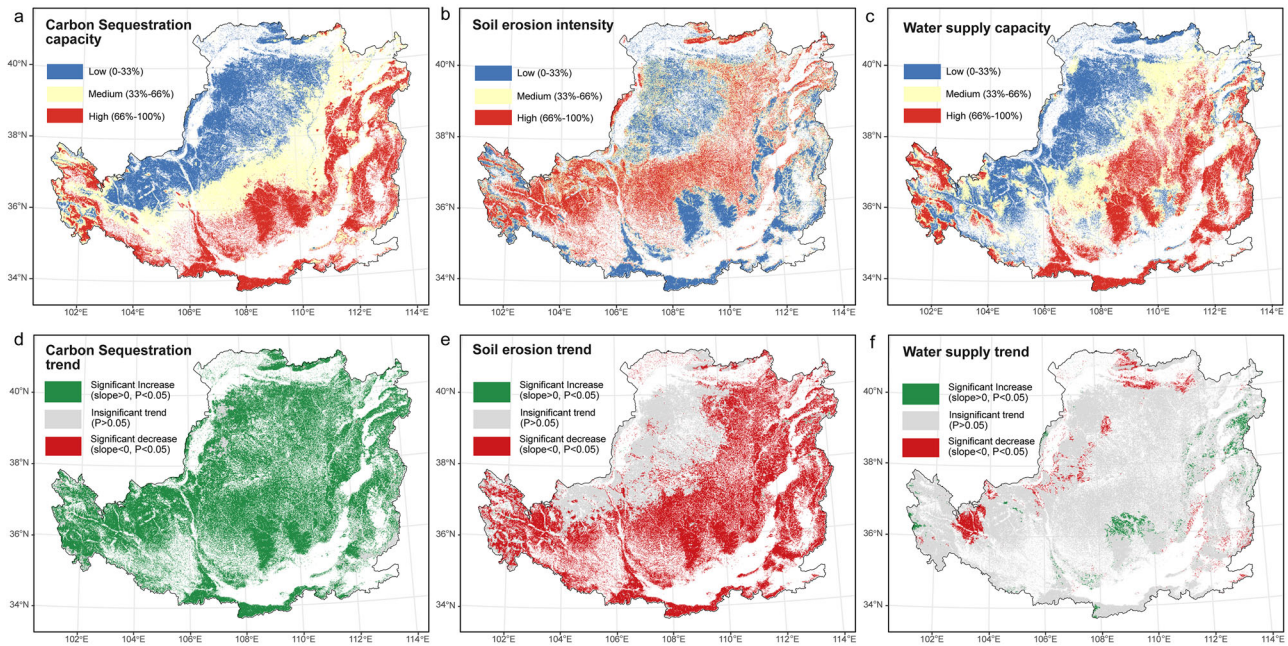


**Fig. 3 | Spatial patterns and temporal trends of ecosystem services on the Loess Plateau.** **a** Carbon sequestration capacity, **b** Soil erosion intensity, **c** Water supply capacity, classified into low (blue), medium (yellow), and high (red) levels. **d** Carbon sequestration trend, **e** Soil erosion trend, **f** Water supply trend, classified into significant decrease (green), significant increase (red), and insignificant trend (gray).

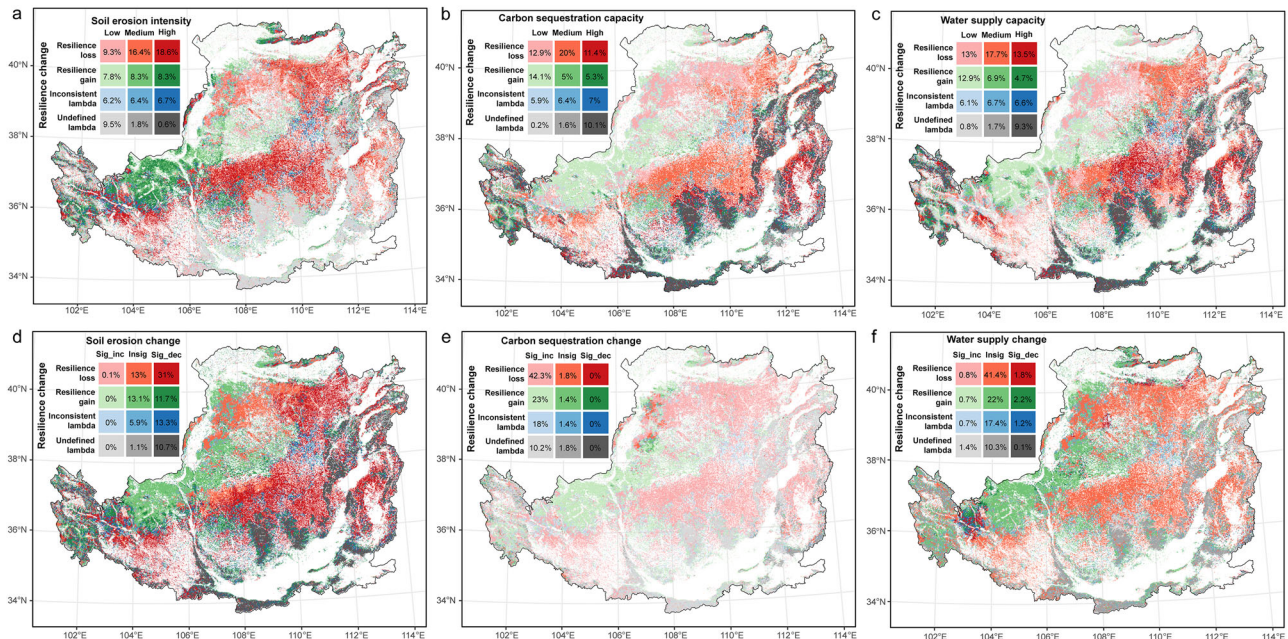


**Fig. 4 | Spatial overlay between ecological resilience and ecosystem services on the Loess Plateau.** **a–c** Spatial overlay of resilience change with ecosystem service supply levels, including soil erosion intensity, carbon sequestration capacity, and water supply capacity. **d–f** Spatial overlay of resilience change with ecosystem service trends, including soil erosion change, carbon sequestration change, and water supply change. The numbers shown in the matrices represent the percentage of the study area corresponding to each overlay category. Sig\_inc, Insig, Sig\_dec are significant increase, insignificant trend, and significant decrease, respectively.

intensity is highest in the central Loess Plateau (Fig. 3b), where sandy and coarse-textured soils are highly susceptible to erosion.

**Spatial coupling of ecological resilience and ecosystem services**

Spatial overlay between ecological resilience and ecosystem services revealed nuanced patterns that were not captured when considering either dimension alone. In areas with high soil erosion intensity (i.e., low soil retention),

18.6% exhibited resilience loss, compared with only 8.3% showing resilience gain (Fig. 4a). Similarly, in regions with high carbon sequestration and water supply capacity, resilience gains were relatively low (5.3% and 4.7%, respectively), whereas resilience loss occurred in 11.4% and 13.5% of the areas (Fig. 4b–c). These results suggest that even well-functioning ecosystems—characterized by high levels of ecosystem service provision—can remain vulnerable to resilience loss and stability decline.

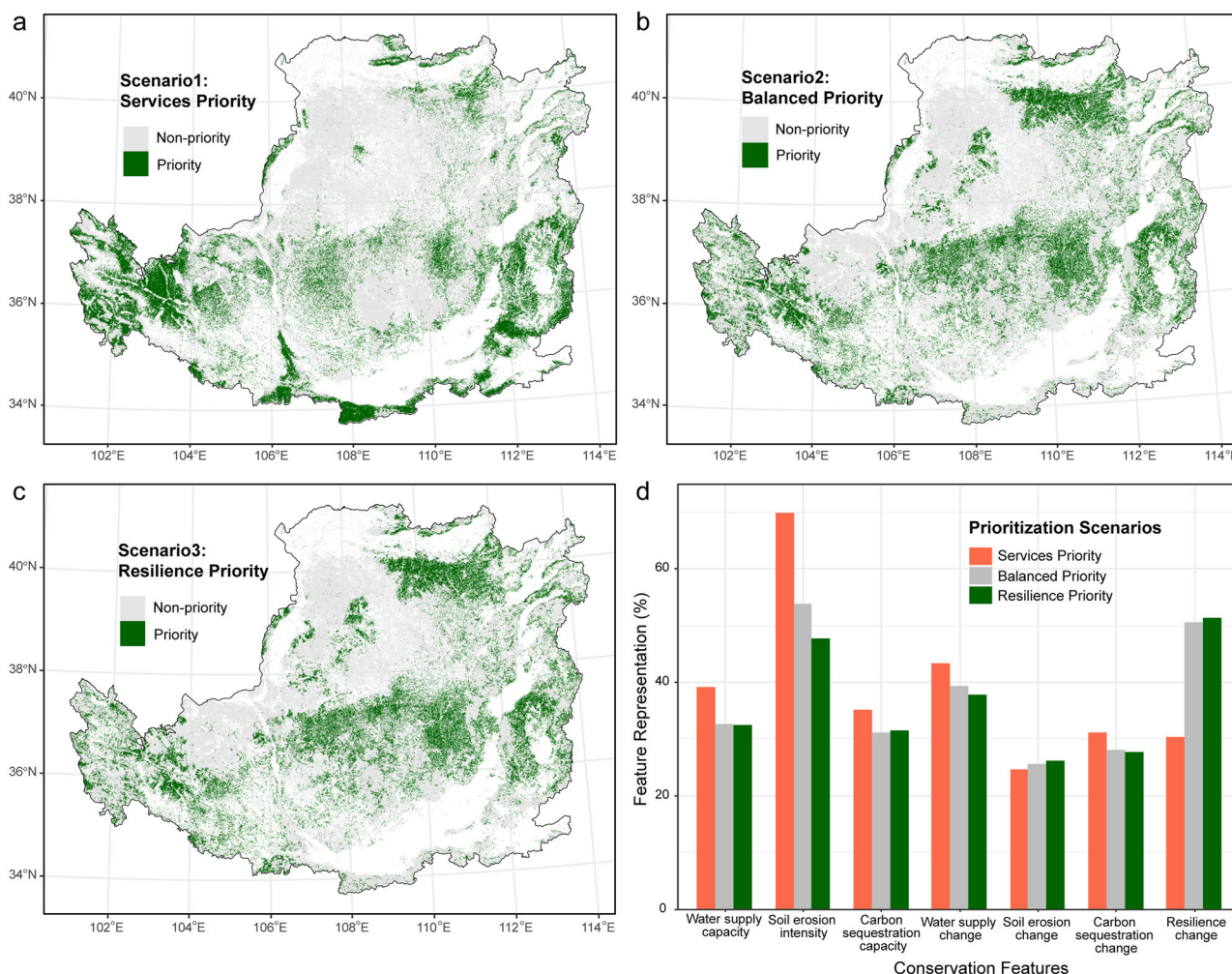


**Fig. 5 | Comparison of priority areas and feature representation across prioritization scenarios. a–c** Spatial distribution of identified priority areas under the Service Priority, Balanced Priority, and Resilience Priority scenarios, respectively. **d** Comparison of feature representation achieved under the three scenarios.

Combined trends of ecosystem services and resilience further highlight potential mismatches between ecosystem service improvements and resilience changes (Fig. 4d–f). For example, in areas where soil erosion significantly decreased, 31% still experienced resilience loss, whereas only 11.7% showed simultaneous improvements in both soil conservation and resilience (Fig. 4d). Similarly, among areas with significant increases in carbon sequestration, 42.3% still exhibited resilience loss, while 23% showed co-increasing trends in both carbon sequestration and resilience (Fig. 4e). In contrast, most regions showed non-significant trends in water supply (Fig. 3f), limiting the detection of direct relationships. Nevertheless, 0.8% of the area experienced resilience loss despite increasing water supply, and 1.8% showed concurrent declines in both variables (Fig. 4f).

**Mapping conservation and restoration priority areas under scenarios**

Spatial patterns of priority areas and their corresponding feature representations varied among the three prioritization scenarios (Fig. 5). Under the Service Priority scenario, priority areas were mainly concentrated in the southern Loess Plateau (Fig. 5a), where ecosystem service supply capacity is relatively high but water supply has locally declined (Fig. 3f). The Balanced Priority and Resilience Priority scenarios exhibited broadly similar spatial patterns (Fig. 5b, c), with priority areas mainly distributed across the central and northern Loess Plateau. These areas are characterized by moderate to high levels of ecosystem service supply (Fig. 3a–c) but face high soil erosion vulnerability (Fig. 3b) and widespread resilience decline (Fig. 2d).

Feature representation revealed clear spatial trade-offs between ecosystem service supply and resilience across the three scenarios (Fig. 5d). Specifically, the Service Priority scenario achieved the highest representation of ecosystem services—particularly for soil erosion intensity (69.1%) and water supply capacity (39.1%)—but showed comparatively low representation of ecological resilience (30.4%). In contrast, the Resilience Priority scenario substantially improved resilience representation (51.4%) while maintaining moderate levels of ecosystem service representation. The Balanced Priority scenario produced intermediate results, with a feature representation pattern closely resembling that of the Resilience Priority case.

**Discussion**

This study contributes a methodological advance by integrating CSD-based resilience assessment, ecosystem service quantification, and spatial conservation optimization into a unified framework (Fig. 1). Unlike conventional approaches that typically focus on maximizing ecosystem service supply alone, this framework enables the identification of regions where ecosystem services are both highly valuable and increasingly vulnerable due to declining resilience, thereby providing a more comprehensive basis for ecosystem management<sup>15</sup>.

Our findings reveal that although ecosystem services on the Loess Plateau have improved significantly over the past two decades (Fig. 3), ecological resilience has not followed a continuous upward trend (Fig. 2). Instead, we identified a clear turning point, where the overall trajectory shifted from increasing to declining resilience (Fig. 2c). This pattern aligns

with previous studies in the region, despite differences in datasets and preprocessing methods, demonstrating the robustness of this resilience estimate<sup>31,32</sup>. Similar transitions in resilience have also been reported in other ecosystems, including the Amazon rainforest<sup>33,34</sup> and global terrestrial vegetation<sup>35,36</sup>, suggesting that resilience decline may be a widespread phenomenon. Because declining resilience reflects an increasing vulnerability of ecosystems to critical transitions in response to external disturbances, this emerging pattern underscores the urgent need to strengthen resilience-oriented management and restoration strategies<sup>2,3</sup>.

By overlaying trends in ecosystem services and resilience, we revealed spatial mismatches that are not apparent when examining either dimension alone (Fig. 4). For instance, 42.3% of the areas showing increased carbon sequestration capacity also exhibited declining resilience (Fig. 4e). This mismatch can be partly explained by the fundamental difference in what these two types of indicators capture. Ecosystem services—such as carbon sequestration or soil conservation—primarily describe the mean state or capacity of ecosystem functions<sup>30</sup>, whereas resilience derived from CSD indicators reflects the higher-order statistical characteristics that respond more sensitively to destabilization<sup>33</sup>. Recognizing this conceptual distinction is crucial for understanding the potential decoupling between ecosystem functioning and stability in regions undergoing rapid ecological restoration.

Beyond this conceptual distinction, the observed mismatch may be explained by three non-exclusive ecological mechanisms. First, in the central Loess Plateau—where semi-arid and semi-humid zones converge and water availability is highly variable—extensive vegetation greening has substantially increased evapotranspiration and water consumption, intensifying carbon–water trade-offs<sup>24</sup>. Ecosystems may initially gain resilience from enhanced productivity, but this benefit diminishes as soil moisture becomes increasingly depleted and locked within vegetation, weakening their capacity to buffer climatic fluctuations<sup>37</sup>. Recent studies have reported that about 17.15% of greening areas in China's drylands face hydrological unsustainability driven by excessive evapotranspiration<sup>38</sup>. Although vegetation greening may enhance regional rainfall via atmospheric moisture recycling<sup>39–41</sup>, the overall water supply–demand balance remains uncertain and warrants further investigation. Second, large-scale restoration on the Loess Plateau has often relied on single-species plantations and simplified vegetation structures, leading to structural homogenization and reduced functional and response diversity<sup>42</sup>. Such simplification increases intra-community competition<sup>43</sup> and weakens the ecosystem's capacity to buffer external disturbances, thereby compromising long-term ecosystem stability<sup>44,45</sup>.

Third, gradual climatic and environmental pressures—such as rising temperature, more frequent droughts, and greater precipitation variability—can further erode system stability<sup>34,46</sup>. For instance, recent evidence suggests that increased temperature and precipitation variability contributed to the resilience decline observed during 2011–2020 on the Loess Plateau<sup>31</sup>. Collectively, these findings highlight that both internal restoration processes and external climatic forces interact to shape the observed service–resilience decoupling. Future research should therefore quantify the relative importance and feedbacks of these mechanisms to advance a more comprehensive understanding of how ecological restoration, water constraints, and climate variability jointly regulate ecosystem resilience.

The spatial and feature representation differences among the three prioritization scenarios reveal clear trade-offs between maximizing ecosystem service supply and maintaining ecosystem resilience. Compared with the Service Priority scenario, the Balanced Priority and Resilience Priority scenarios emphasize ecosystems in the central and northern Loess Plateau, which exhibit moderate levels of ecosystem services but higher vulnerability to soil erosion and resilience loss (Fig. 5). These areas represent potential ecological management hotspots, where conservation actions should focus not only on sustaining service provision but also on preventing further resilience loss. Identifying such priority areas provides a spatially explicit basis for reconciling short-term functional gains with long-term ecosystem stability.

To enhance both ecosystem service supply and resilience, restoration efforts should adopt resilience-based strategies that integrate structural and functional diversity, water–carbon balance, and adaptive management. In water-limited regions such as the central Loess Plateau, this entails reducing over-dense stands, optimizing species composition, and restoring mixed grass–shrub–tree mosaics to alleviate water stress and improve drought resistance<sup>42,45,47</sup>. Forest management practices such as appropriate thinning can mitigate soil water depletion and improve water sustainability, thereby preventing potential declines in ecosystem resilience<sup>47</sup>. Furthermore, promoting native and multi-species plantations instead of single-species forests can increase functional redundancy and enhance adaptive capacity<sup>42,44</sup>. Evidence from Amazon and European forest further suggests that higher tree diversity and structural diversity can dampen critical slowing down, promoting faster recovery from disturbances and improving long-term stability<sup>48,49</sup>. Such regionally differentiated and evidence-informed strategies would enable managers to sustain ecosystem service gains without compromising resilience, ensuring the long-term ecological sustainability of the Loess Plateau.

While this study presents an integrated framework that combines ecosystem service supply and ecosystem resilience in spatial conservation prioritization, several methodological and practical limitations remain. The CSD-based resilience assessment still carries methodological uncertainties, as its robustness depends on the quality, length, and stationarity of the time series<sup>5</sup>. Vegetation indices such as kNDVI, while effective proxies for canopy dynamics, may saturate in dense vegetation, potentially underestimating resilience in high-biomass regions such as forests<sup>29</sup> (Fig. 2d). Moreover, this study focused primarily on biophysical dimensions and did not explicitly incorporate socio-economic costs, land-use feasibility, or stakeholder preferences, which are essential for translating spatial priorities into actionable management<sup>10,13</sup>. Specifically, a uniform cost of 1 was assigned to all planning units to highlight the trade-offs between ecosystem services and resilience, without accounting for actual implementation constraints. Future research should integrate spatially explicit socio-economic data, restoration costs, and stakeholder perspectives to improve the practical applicability and policy relevance of the proposed framework.

## Methods

### Study area

To minimize the influence of anthropogenic land use and land-cover conversion on resilience assessments, we restricted our analysis to non-converted vegetated lands (grasslands and forests) that remained stable between 2000 and 2020 (Supplementary Fig. 1). Land-cover data were obtained from Yang & Huang<sup>50</sup>, originally at 30 m spatial resolution and resampled to 1 km. Farmland pixels were excluded because their vegetation dynamics are strongly influenced by intensive human management practices—such as irrigation, fertilization, and harvesting—which can obscure natural recovery signals and bias the estimation of resilience indicators<sup>29</sup>.

### Data preprocessing

The kernel normalized difference vegetation index (kNDVI) was used as a proxy for vegetation state. It shows stronger correspondence with primary productivity and improved robustness to saturation, bias, and noise across space and time compared with conventional indices such as NDVI and near-infrared reflectance of vegetation (NIRv)<sup>51</sup>. Monthly MODIS NDVI data (MOD13A3.061, 1 km) from February 2000 to December 2023 were transformed to kNDVI using the Eq. (1)<sup>52</sup>. Only pixels with continuous kNDVI time series were retained for subsequent resilience estimation.

$$kNDVI = \tanh(NDVI^2) \quad (1)$$

To obtain stationary residuals suitable for CSD analysis, long-term trends and seasonal cycles were removed following Smith & Boers (2023)<sup>29</sup>. Specifically, a 5-year rolling mean was first applied to remove long-term

trends, followed by harmonic fitting to remove seasonal components<sup>29</sup>. The resulting residuals represent high-frequency ecosystem fluctuations around a quasi-equilibrium state.

### Measuring ecological resilience

Ecological resilience was quantified using recovery rates derived from critical slowing down (CSD) indicators<sup>28</sup>. Theoretically, when an ecosystem approaches a critical threshold, its ability to recover from perturbations slows down<sup>3</sup>. This dynamic can be approximated by a linearized stochastic differential equation describing small deviations around a quasi-equilibrium state<sup>29</sup>:

$$dX_t = \lambda X_t dt + \sigma dW_t \quad (2)$$

Where  $X_t$  represents deviations from the equilibrium.  $\lambda$  ( $\lambda < 0$  for stable dynamics) denotes the recovery rate,  $\sigma$  the volatility, and  $W_t$  a Wiener process representing stochastic perturbations. As the system loses resilience,  $\lambda$  increases toward zero from below, indicating slower recovery.

To apply this continuous-time formulation to discrete satellite-based time series, Eq. (2) can be discretized into a first-order autoregressive process<sup>29</sup>:

$$X_{n+1} = aX_n + \tilde{\sigma}\eta_n \quad (3)$$

In practice, two recovery rate estimates were derived: one based on lag-1 autocorrelation ( $\lambda_{AC1}$ ) and the other based on variance ( $\lambda_{var}$ ) of the kNDVI residuals. The corresponding formulations are<sup>29</sup>:

$$\lambda_{AC1} = \frac{\log(a)}{\Delta t} \quad (4)$$

$$\lambda_{var} = \frac{1}{2\Delta t} \log\left(1 - \frac{\tilde{\sigma}^2}{Var[X]}\right) \quad (5)$$

Where  $a$  is the lag-1 autocorrelation,  $\tilde{\sigma}^2$  the noise variance, and  $Var[X]$  the total variance of the time series. Both indicators theoretically yield consistent estimates of recovery rate under stable system dynamics<sup>29,36</sup>.

Two  $\lambda$  estimates ( $\lambda_{AC1}$  and  $\lambda_{var}$ ) were computed within a 5-year rolling window using the kNDVI residuals, and the temporal trends of  $\lambda$  were quantified via Kendall's tau statistic to infer the direction and significance of resilience change. Following Smith and Boers<sup>39</sup>, resilience change was classified into four categories: Resilience loss,  $\lambda$  increasing significantly in both estimators; Resilience gain,  $\lambda$  decreasing in both; Inconsistent trend, opposite signs; Undefined  $\lambda$ , due to negative AC1 or the ratio of process noise variance to total variance exceeded 1. To test robustness, alternative window settings were applied (3–5 years for detrending and 5–7 years for  $\lambda$  estimation), yielding consistent classification results (Supplementary Figs. 2 and 3).

### Assessing ecosystem services

This study quantified three key vegetation-related ecosystem services—soil conservation, carbon sequestration, and water supply—using well-established and validated approaches<sup>30</sup>.

Soil erosion from 2000 to 2020 was estimated using the Universal Soil Loss Equation (USLE), which integrates multiple biophysical factors, including rainfall erosivity, soil erodibility, slope length and steepness, vegetation cover, and land management practices<sup>53</sup>. Model outputs were validated against observed sediment load data from hydrological monitoring stations along the Yellow River, confirming their reliability for regional-scale application<sup>30</sup>. Carbon sequestration from 2000 to 2020 was represented by net primary productivity (NPP) derived from the MODIS MOD17-A3HGF product (500 m resolution), providing a consistent and spatially explicit proxy for ecosystem carbon uptake. Water supply from 2001 to 2020 was derived from a water balance approach, defined as precipitation minus

actual evapotranspiration<sup>54</sup>. The estimates were validated against observed runoff data from representative catchments across the Loess Plateau, demonstrating their robustness for spatial analysis<sup>30</sup>.

To characterize spatial heterogeneity, the multi-year mean of each ecosystem service was classified into three levels based on quantile thresholds: Low (0–33%), Medium (33%–66%), and High (66%–100%). Temporal trends were quantified using Sen's slope estimator combined with the Mann-Kendall test and categorized as significant increase (slope > 0,  $P < 0.05$ ), significant decrease (slope < 0,  $P < 0.05$ ), and no significant trend ( $P > 0.05$ )<sup>30</sup>.

The one-year offset of the water supply data relative to the other two services arises from the temporal coverage of the underlying evapotranspiration dataset, which begins in February 2000, making 2001 the first complete year available for annual estimation<sup>55</sup>. To ensure that this offset did not bias the integrated analysis, additional sensitivity tests were performed by recalculating soil conservation and carbon sequestration for the overlapping period (2001–2020) (Supplementary Fig. 4–6). The spatial patterns and temporal trends of both indicators remained nearly identical to those derived for 2000–2020 (Supplementary Fig. 4–5), with pixel-wise correlations exceeding 0.98 ( $P < 0.001$ ) (Supplementary Fig. 6). These results confirm that the absence of 2000 data in the water supply assessment introduces negligible spatial or temporal bias and does not affect the overall service–resilience coupling analysis.

### Prioritizing conservation areas under scenarios

Spatial conservation priorities were identified using the R package *prioritizr*, which performs spatially explicit conservation planning based on mixed integer linear programming (MILP) techniques<sup>56</sup>. Seven raster-based features were incorporated into the prioritization framework, grouped into three dimensions:

(1) Ecosystem service supply capacity, including carbon sequestration capacity, water supply capacity, and soil erosion intensity, quantified as multi-year averages. Areas with higher water supply and carbon sequestration capacity, as well as more severe soil erosion intensity, were assigned a higher conservation priority.

(2) Ecosystem service trends, including temporal changes in carbon sequestration, water supply, and soil erosion. Areas showing degradation trends were prioritized. To emphasize degradation, Sen's slope estimates for carbon sequestration and water supply were inverted and weighted by their statistical significance (P-value) as: Weighted value =  $(-slope + \max(-slope)) \times (1 - P)$ , where higher values represent stronger degradation trends. For soil erosion, since an increasing trend indicates worsening conditions, slopes were not inverted but weighted as: Weighted value =  $(slope + \max(slope)) \times (1 - P)$ , where higher values indicate more severe erosion trends.

(3) Ecological resilience change, categorized into Resilience loss, Inconsistent trend, Undefined, and Resilience gain, with assigned scores of 10, 7, 5, and 3, respectively. Higher scores reflected greater management urgency.

To reduce the influence of extreme values, raster outliers were clipped at the upper and lower 5% quantiles. All feature layers were normalized to a 0–1 scale to ensure comparability across indicators and integration within the prioritization model.

To explore potential trade-offs between ecosystem services and ecological resilience in conservation planning, three prioritization scenarios were designed and compared (Table 1). A uniform cost surface (cost=1) was assigned to all planning units to ensure that prioritization outcomes were driven solely by feature values rather than cost variability. A maximal feature representation objective was applied under a 30% area constraint, simulating realistic land use limitations. Three alternative weighting schemes were implemented using the `add_feature_weights()` function in *prioritizr* package, allowing systematic adjustment of the relative importance of ecosystem services and resilience across scenarios<sup>56</sup>. A binary decision model was adopted, where each planning unit (raster cell) was either selected or not. The HiGHS solver was used to solve the MILP optimization

**Table 1 | The three prioritization scenarios based on ecosystem service and resilience weight settings**

Scenario	Description	Feature Weights	Implication
Service Priority	Focuses solely on ecosystem services, ignoring resilience.	Services=1 (each service 1/6 × 6 service features); Resilience=0	Maximizes ecosystem services but risks overlooking long-term ecological resilience.
Balanced Priority	Balances ecosystem services and resilience equally.	Services=1/2 (each service 1/12 × 6 service features); Resilience=1/2	Achieves a balance between short-term functionality and long-term resilience.
Resilience Priority	Prioritizes ecological resilience over ecosystem services.	Services = 1/3 (each service 1/18 × 6 service features); Resilience = 2/3	Enhance ecological resilience, with moderate service representation.

problem for each scenario<sup>57</sup>, and the resulting solution rasters were interpreted as the spatial distribution of conservation priority areas under different management strategies.

### Data availability

Monthly NDVI data with a resolution of 1 km from February 2000 to December 2023 were acquired from MODIS (MOD13A3 Version 6.1, <https://www.earthdata.nasa.gov/data/catalog/lpcloud-mod13a3-061>). Land use/cover data with a 30 m resolution in 2000 and 2020 was obtained from Zenodo (<https://zenodo.org/records/15853565>)<sup>58</sup>. The datasets supporting the findings of this study, including ecosystem service and resilience assessment results, have been deposited in figshare and are available at [<https://figshare.com/s/d6d5d65bbd9e77a02441>].

### Code availability

The code used for the study is available from the author’s figshare repository (<https://figshare.com/s/d6d5d65bbd9e77a02441>).

Received: 17 May 2025; Accepted: 20 January 2026;

Published online: 31 January 2026

### References

- Scheffer, M. et al. Early-warning signals for critical transitions. *Nature* **461**, 53–59 (2009).
- Dakos, V. et al. Tipping point detection and early warnings in climate, ecological, and human systems. *Earth Syst. Dynam.* **15**, 1117–1135 (2024).
- Scheffer, M., Carpenter, S. R., Dakos, V. & Van Nes, E. H. Generic Indicators of Ecological Resilience: Inferring the Chance of a Critical Transition. *Annu. Rev. Ecol., Evolution, Syst.* **46**, 145–167 (2015).
- Dakos, V., Carpenter, S. R., van Nes, E. H. & Scheffer, M. Resilience indicators: Prospects and limitations for early warnings of regime shifts. *Philos. Trans. R. Soc. B: Biol. Sci.* **370**, 1–10 (2015).
- Lenton, T. M. et al. Remotely sensing potential climate change tipping points across scales. *Nat. Commun.* **15**, 343 (2024).
- Felipe-Lucia, M. R. et al. Conceptualizing ecosystem services using social–ecological networks. *Trends Ecol. Evolution* **37**, 211–222 (2022).
- Biggs, R., Schlüter, M. & Schoon, M. *Principles for Building Resilience: Sustaining Ecosystem Services in Social–Ecological Systems*. (2015).
- Liu, Y., Kumar, M., Katul, G. G. & Porporato, A. Reduced resilience as an early warning signal of forest mortality. *Nat. Clim. Change* **9**, 880–885 (2019).
- Fernández-Martínez, M. et al. Diagnosing destabilization risk in global land carbon sinks. *Nature* **615**, 848–853 (2023).
- Tallis, H. et al. Prioritizing actions: spatial action maps for conservation. *Ann. N. Y. Acad. Sci.* **1505**, 118–141 (2021).
- Moilanen, A. et al. Novel methods for spatial prioritization with applications in conservation, land use planning and ecological impact avoidance. *Methods Ecol. Evolution* **13**, 1062–1072 (2022).
- Sun, Q. et al. Mapping Biodiversity Conservation Priorities for Protected Areas for Spatial Optimization: A Case Study in the Songnen Plain, China. *Ecol. Evolution* **14**, e70516 (2024).
- Giakoumi, S. et al. Advances in systematic conservation planning to meet global biodiversity goals. *Trends Ecol. Evolution* **40**, 395–410 (2025).
- Standish, R. J. & Parkhurst, T. Interventions for resilient nature-based solutions: An ecological perspective. *J. Ecol.* **112**, 2502–2509 (2024).
- Chambers, J. C., Allen, C. R. & Cushman, S. A. Operationalizing Ecological Resilience Concepts for Managing Species and Ecosystems at Risk. *Frontiers in Ecology and Evolution* **Volume 7 - 2019**, (2019).
- Angeler, D. G. & Allen, C. R. Quantifying resilience. *J. Appl. Ecol.* **53**, 617–624 (2016).
- Runge, K. et al. Monitoring Terrestrial Ecosystem Resilience Using Earth Observation Data: Identifying Consensus and Limitations Across Metrics. *Glob. Change Biol.* **31**, e70115 (2025).
- Lenton, T. M. et al. A resilience sensing system for the biosphere. *Philos. Trans. R. Soc. B: Biol. Sci.* **377**, 20210383 (2022).
- Wang, Z. et al. Escaping social–ecological traps through ecological restoration and socioeconomic development in China’s Loess Plateau. *People Nat.* **5**, 1364–1379 (2023).
- Fu, B., Wu, X., Wang, Z., Wu, X. & Wang, S. Coupling human and natural systems for sustainability: experience from China’s Loess Plateau. *Earth Syst. Dyn.* **13**, 795–808 (2022).
- Wu, X. et al. Ecological restoration in the Yellow River Basin enhances hydropower potential. *Nat. Commun.* **16**, 2566 (2025).
- Lü, Y., Lü, D., Feng, X. & Fu, B. Multi-scale analyses on the ecosystem services in the Chinese Loess Plateau and implications for dryland sustainability. *Curr. Opin. Environ. Sustainability* **48**, 1–9 (2021).
- Wu, X., Wang, S., Fu, B., Feng, X. & Chen, Y. Socio-ecological changes on the Loess Plateau of China after Grain to Green Program. *Sci. Total Environ.* **678**, 565–573 (2019).
- Feng, X. et al. Revegetation in China’s Loess Plateau is approaching sustainable water resource limits. *Nat. Clim. Change* **6**, 1019–1022 (2016).
- Zhang, S. et al. Excessive Afforestation and Soil Drying on China’s Loess Plateau. *J. Geophys. Res.: Biogeosciences* **123**, 923–935 (2018).
- Potschin-Young, M. et al. Understanding the role of conceptual frameworks: Reading the ecosystem service cascade. *Ecosyst. Serv.* **29**, 428–440 (2018).
- Mandle, L. et al. Increasing decision relevance of ecosystem service science. *Nat. Sustainability* **4**, 161–169 (2021).
- Dakos, V. & Kéfi, S. Ecological resilience: what to measure and how. *Environ. Res. Lett.* **17**, 043003 (2022).
- Smith, T. & Boers, N. Reliability of vegetation resilience estimates depends on biomass density. *Nat. Ecol. Evolution* **7**, 1799–1808 (2023).
- Wang, Z. et al. Exploring the interdependencies of ecosystem services and social-ecological factors on the Loess Plateau through network analysis. *Sci. Total Environ.* **960**, 178362 (2025).
- Wang, Z. et al. Vegetation resilience does not increase consistently with greening in China’s Loess Plateau. *Commun. Earth Environ.* **4**, 336 (2023).

32. Zhang, Y. et al. Spatial Heterogeneity of Vegetation Resilience Changes to Different Drought Types. *Earth's Future* **11**, e2022EF003108 (2023).
33. Boulton, C. A., Lenton, T. M. & Boers, N. Pronounced loss of Amazon rainforest resilience since the early 2000s. *Nat. Clim. Change* **12**, 271–278 (2022).
34. Van Passel, J. et al. Critical slowing down of the Amazon forest after increased drought occurrence. *Proc. Natl. Acad. Sci.* **121**, e2316924121 (2024).
35. Feng, Y. et al. Reduced resilience of terrestrial ecosystems locally is not reflected on a global scale. *Commun. Earth Environ.* **2**, 88 (2021).
36. Smith, T., Traxl, D. & Boers, N. Empirical evidence for recent global shifts in vegetation resilience. *Nat. Clim. Change* **12**, 477–484 (2022).
37. Liu, Y. et al. Global greening drives significant soil moisture loss. *Commun. Earth Environ.* **6**, 600 (2025).
38. Fu, F. et al. Locating Hydrologically Unsustainable Areas for Supporting Ecological Restoration in China's Drylands. *Earth's Future* **12**, e2023EF004216 (2024).
39. Wei, F. et al. Quantifying the precipitation supply of China's drylands through moisture recycling. *Agric. For. Meteorol.* **352**, 110034 (2024).
40. Tian, L. et al. Large-Scale Afforestation Enhances Precipitation by Intensifying the Atmospheric Water Cycle Over the Chinese Loess Plateau. *J. Geophys. Res.: Atmospheres* **127**, e2022JD036738 (2022).
41. Cui, J. et al. Global water availability boosted by vegetation-driven changes in atmospheric moisture transport. *Nature Geoscience*, <https://doi.org/10.1038/s41561-022-01061-7> (2022).
42. Zhao, Y. et al. Beyond monocultures: Optimizing soil carbon sequestration with diverse planting strategies on the Loess Plateau. *CATENA* **246**, 108447 (2024).
43. Zhang, J. et al. Plant water source and water niche of native typical communities in the Loess Plateau of China. *Ecol. Front.* **45**, 1582–1594 (2025).
44. Liu, C. L. C., Kuchma, O. & Krutovsky, K. V. Mixed-species versus monocultures in plantation forestry: Development, benefits, ecosystem services and perspectives for the future. *Glob. Ecol. Conserv.* **15**, e00419 (2018).
45. Felton, A. et al. Replacing monocultures with mixed-species stands: Ecosystem service implications of two production forest alternatives in Sweden. *Ambio* **45**, 124–139 (2016).
46. Smith, T. & Boers, N. Global vegetation resilience linked to water availability and variability. *Nat. Commun.* **14**, 498 (2023).
47. Liu, Y. et al. Effects of thinning on soil water content and water use characteristics of artificial forest in the Loess Plateau of China. *CATENA* **254**, 108997 (2025).
48. Van Passel, J. et al. Higher tree diversity reduces critical slowing down in the Amazon forest. *EGUsphere* **2025**, 1–31, (2025).
49. Pickering, M. et al. Enhanced structural diversity increases European forest resilience and potentially compensates for climate-driven declines. *Commun. Earth Environ.* **6**, 852 (2025).
50. Yang, J. & Huang, X. The 30 m annual land cover dataset and its dynamics in China from 1990 to 2019. *Earth Syst. Sci. Data* **13**, 3907–3925 (2021).
51. Camps-Valls, G. et al. A unified vegetation index for quantifying the terrestrial biosphere. *Sci. Adv.* **7**, eabc7447 (2021).
52. Forzieri, G., Dakos, V., McDowell, N. G., Ramdane, A. & Cescatti, A. Emerging signals of declining forest resilience under climate change. *Nature* **608**, 534–539 (2022).
53. Fu, B. et al. Assessing the soil erosion control service of ecosystems change in the Loess Plateau of China. *Ecol. Complex.* **8**, 284–293 (2011).
54. Su, C., Dong, M., Fu, B. & Liu, G. Scale effects of sediment retention, water yield, and net primary production. A case-study of the Chinese Loess Plateau. *Land Degrad. Dev.* **31**, 1408–1421 (2020).
55. Zhang, Y. & He, S. PML-V2 (China): evapotranspiration and gross primary production dataset (2000.02.26–2020.12.31). National Tibetan Plateau/Third Pole Environment Data Center (2022).
56. Hanson, J. O. et al. Systematic conservation prioritization with the prioritizr R package. *Conserv. Biol.* **39**, e14376 (2025).
57. Huangfu, Q. & Hall, J. A. J. Parallelizing the dual revised simplex method. *Math. Program. Comput.* **10**, 119–142 (2018).
58. Yang, J. & Huang, X. The 30 m annual land cover datasets and its dynamics in China from 1990 to 2020 (1.0.4) [Data set]. *Zenodo*. <https://doi.org/10.5281/zenodo.5210928> (2021).

## Acknowledgements

This study was supported by the National Natural Science Foundation of China (42501114, W2412141), the Fundamental Research Funds for the Central Universities (GK202506004), Young Talent Fund of Xi'an Association for Science and Technology (0959202513114).

## Author contributions

B.F. and Z.W. conceived and designed the study. Z.W. produced and analyzed the results and led the writing of the manuscript. B.F., X.W., S.W., J.Z., L.Z., L.J., H.W., Y.L., and Y.L. commented and edited the manuscript. All authors contributed to interpreting the results and improving the paper.

## Competing interests

The authors declare no competing interests.

## Additional information

**Supplementary information** The online version contains supplementary material available at <https://doi.org/10.1038/s43247-026-03244-1>.

**Correspondence** and requests for materials should be addressed to Bojie Fu.

**Peer review information** *Communications Earth & Environment* thanks Xiangyang Hou and the other, anonymous, reviewer(s) for their contribution to the peer review of this work. Primary Handling Editors: Leticia Santos de Lima and Mengjie Wang. A peer review file is available

**Reprints and permissions information** is available at <http://www.nature.com/reprints>

**Publisher's note** Springer Nature remains neutral with regard to jurisdictional claims in published maps and institutional affiliations.

**Open Access** This article is licensed under a Creative Commons Attribution-NonCommercial-NoDerivatives 4.0 International License, which permits any non-commercial use, sharing, distribution and reproduction in any medium or format, as long as you give appropriate credit to the original author(s) and the source, provide a link to the Creative Commons licence, and indicate if you modified the licensed material. You do not have permission under this licence to share adapted material derived from this article or parts of it. The images or other third party material in this article are included in the article's Creative Commons licence, unless indicated otherwise in a credit line to the material. If material is not included in the article's Creative Commons licence and your intended use is not permitted by statutory regulation or exceeds the permitted use, you will need to obtain permission directly from the copyright holder. To view a copy of this licence, visit <http://creativecommons.org/licenses/by-nc-nd/4.0/>.

© The Author(s) 2026